An Intelligent Relay Node Selection Scheme in Space-Air-Ground Integrated Networks

Feng Wang[1], Dingde Jiang[1](✉), Jiang Zhu[2], and Zuoliang Liu[2]

[1] School of Astronautics and Aeronautic, UESTC, Chengdu 611731, China
jiangdd@uestc.edu.cn
[2] School of Communication and Information Engineering, CUPT, Chongqing 400065, China

Abstract. The Space-air-ground integrated network (SAGIN) has been a valuable architecture for communication support due to its characteristics of wide coverage and low transmission delay. Both low earth orbit (LEO) satellites and UAVs can serve as relay nodes to provide reliable communication services for ground devices. However, the design of relay node selection scheme in SAGIN is not easy, considering different accessing layers and resource usage of network segments. Moreover, network topology, available resources and relative motion need to be analyzed comprehensively. To address these problems, a traffic prediction method based on autoregressive moving average (ARMA) model is utilized firstly to forecast the resource usage of SAGIN segments. After the analysis of link performance, the Adaboost algorithm is used to classify network nodes for optimal relay node selection. Simulation results show that the proposed intelligent relay node selection scheme is feasible and effective.

Keywords: Space-air-ground integrated network · Traffic prediction · Adaboost model · Relay node selection

1 Introduction

Utilizing ultramodern communication technologies and interconnecting space, air, ground network segments, the space-air-ground integrated network (SAGIN) has attracted many attentions from academia to industry [1]. LEO constellation has the advantages of low delay, high capacity, full coverage and manageability. DJI, the world leader in UAVs and aerial photography technology, has exhibited its new SkyCells communication solutions to optimize the current ground network. The UAV and LEO satellite networks can extend network coverage in highly congested city areas. The UAV and LEO satellite node will serve as the relay node to help transmit data among the ground devices. However, in the LEO satellite layer and air vehicle layer, the segments move at a high speed and the network topology is constantly changing [2]. As a result, the network performance, such as network traffic, link delay, bandwidth, and connection time, will change sequentially with the movement of segments, which causes difficulties in the selection of relay nodes [3]. Meanwhile, the ground device is always covered by multiple UAVs and LEO satellites. How to choose

H. Song et al. (Eds.): SIMUtools 2019, LNICST 295, pp. 157–167, 2019.
https://doi.org/10.1007/978-3-030-32216-8_15

the appropriate accessing node according to the communication requirements to ensure the load balance of the integrated network also needs to be considered [4].

In recent years, more and more researchers have been starting their projects on traffic prediction, network control and path planning in SAGIN. Authors in [5] tried to combine wavelet transform and autoregressive integrated moving average (ARIMA) algorithm to predict self-similar traffic in satellite-ground networks. The self-similarity of satellite network traffic is proved. In general, the SAGIN can be modeled with a directed connected graph for network analysis and control. Authors in [6] mainly considered the link planning from small satellite networks (SSNs) to ground devices. An extended time-evolving graph was exploited to characterize the network resources. The network profit was formulated as a mixed-integer linear programming model. Authors in [7] developed a new dynamic CPD algorithm while considering the time-varying property of contacts in broadband data relay satellite networks. The flow optimization problem in the time-spread graph was treated as a random optimization problem. The relay selection algorithm could improve the throughput, but the computational complexity of the proposed scheme was high, which could occupy more network resources. Most methods above did not consider the computational complexity of the scheme. A lightweight relay node scheme needs to be designed, considering the dynamic topology of SAGIN. Traffic modeling [8], traffic estimation [9], network selection [10], energy efficiency [11] and network behaviors [12] are studied in previous work.

In this paper, the network traffic is considered as an important reference because it can reflect the current load of network segments. Therefore, a network traffic prediction scheme based on ARMA model is utilized to evaluate the node performance. Furthermore, the network performance metrics such as link delay, bandwidth and connection time are all take into consideration for segment evaluation. In order to realize fast relay node selection, an Adaboost based link planning (ALP) algorithm is proposed. All relay nodes are divided into 4 levels according to their data transmission capacity (DTC). As a result, devices with different communication requirements can be assigned to the optimal relay nodes, and the load balance of the SAGIN network is also improved.

The rest of this paper is organized as follows. Section 2 constructs the mathematical model of ARMA for traffic prediction of SAGIN and then proposes the ALP algorithm. The simulation results and analysis are shown in Sect. 3. We then conclude our work in Sect. 4.

2 Mathematical Model

In this section, we mainly talk about network performance evaluation of space-air-ground integrated network (SAGIN). Firstly, a traffic prediction method based on autoregressive moving average (ARMA) model is utilized to forecast the resource usage of SAGIN segments. After the analysis of link performance, the Adaboost-algorithm is used to classify network nodes according to their data transmission capacity. Then, an Adaboost-based link planning (ALP) algorithm is proposed for relay node selection.

The $ARMA(p, q)$ model is a commonly used time series model to realize the optimal traffic prediction. By analyzing the structure and characteristics of time series, the minimum variance is obtained. The $ARMA(p, q)$ model is composed of the $AR(p)$ and $MA(q)$ models. The $AR(p)$ model utilizes a linear combination of present disturbance data and past observation data for traffic prediction, which can be formulated as follows:

$$X_t = \alpha_1 X_{t-1} + \alpha_2 X_{t-2} + \cdots + \alpha_p X_{t-p} + \xi_t \tag{1}$$

X_t is the time series and $\alpha_i (i = 1, 2, \cdots, p)$ are the undetermined coefficients of the $AR(p)$ model. p is the order of $AR(p)$, and the prediction error is denoted by ξ_t. The $MA(q)$ model makes use of a linear combination of present and past disturbance data to help traffic prediction. The model can be described as:

$$u_t = \varepsilon_t - \beta_1 \varepsilon_{t-1} - \beta_2 \varepsilon_{t-2} - \cdots - \beta_q \varepsilon_{t-q} \tag{2}$$

where u_t is the observed value, $\varepsilon_i (i = t-q, t-q+1, \cdots, t)$ are the prediction errors of the X_i, and q is the order of $MA(q)$. $\beta_i (i = 1, 2, \cdots, q)$ are the undetermined coefficients. As a result, $ARMA(p, q)$ is a combination of $AR(p)$ and $MA(q)$, which can be expressed as:

$$\begin{aligned} X_t &= \alpha_1 X_{t-1} + \alpha_2 X_{t-2} + \cdots + \alpha_p X_{t-p} \\ &+ \varepsilon_t - \beta_1 \varepsilon_{t-1} - \beta_2 \varepsilon_{t-2} - \cdots - \beta_q \varepsilon_{t-q} \end{aligned} \tag{3}$$

In order to utilize the $ARMA(p, q)$ model for traffic prediction, it is necessary to find the best fitting, that is, to determine the order (p, q) and other coefficients. The order (p, q) can be determined by verifying the autocorrelation function (ACF) and partial correlation function (PACF) of the time sequences X_t.The ACF and PACF of X_t can be calculated as ρ_k and Φ_{kk}:

$$\rho_k = \frac{Cov(X_t, X_{t+k})}{\sigma_X^2} \tag{4}$$

$$\Phi_{kk} = \frac{\rho_k - \sum_{i=1}^{k-1} \Phi_{k-1,i} \rho_{k-i}}{1 - \sum_{i=1}^{k-1} \Phi_{k-1,i} \rho_i} \quad k = 2, 3, \ldots \tag{5}$$

Where

$$\Phi_{11} = \rho_1 \tag{6}$$

$$\Phi_{ki} = \Phi_{k-1,i} - \Phi_{kk} \Phi_{k-1,k-1} \tag{7}$$

When the PACF of X_t meets $\Phi_{ki} = 0\ (k > p)$, the value of p is $k - 1$. Similarly, if the ACF of X_t meets $\rho_k = 0\ (k > q)$, the value of q is $k - 1$.

The moment estimation method is used to calculate the coefficients, which has the advantages of simple calculation and high estimation accuracy. Firstly the $ARMA(p, q)$ model can be expressed as:

$$X_t = \sum_{i=1}^{p} \alpha_i X_{t-i} + \varepsilon_t + \sum_{i=1}^{q} \beta_i \varepsilon_{t-i} \tag{8}$$

where $\{\varepsilon_t\}$ is normally distributed as $N(0, \sigma^2)$. α and β meet:

$$\alpha(z) = 1 - \sum_{i=1}^{p} \alpha_i z^i \tag{9}$$

$$\beta(z) = 1 + \sum_{i=1}^{q} \beta_i z^i \tag{10}$$

The $\alpha(z)$ and $\beta(z)$ are prime of each other and meets $\alpha(z)\beta(z) \neq 0,\ |z| \leq 1$. Meanwhile, $\alpha(z)$ can be calculated as:

$$\begin{bmatrix} X_{q+1} \\ X_{q+2} \\ \vdots \\ X_{p+q} \end{bmatrix} = \begin{bmatrix} X_q & X_{q-1} & \cdots & X_{q-p+1} \\ X_{q+1} & X_q & \cdots & X_{q-p+2} \\ \vdots & \vdots & & \vdots \\ X_{q+p-1} & X_{q+p-2} & \cdots & X_q \end{bmatrix} \begin{bmatrix} \alpha_1 \\ \alpha_2 \\ \vdots \\ \alpha_p \end{bmatrix} \tag{11}$$

$\hat{X}_t$ is used to represent the ACF of the time sequences X_t, and the moment estimate value of α can be calculated as follows:

$$\begin{bmatrix} \hat{\alpha}_1 \\ \hat{\alpha}_2 \\ \vdots \\ \hat{\alpha}_p \end{bmatrix} = \begin{bmatrix} \hat{X}_q & \hat{X}_{q-1} & \cdots & \hat{X}_{q-p+1} \\ \hat{X}_{q+1} & \hat{X}_q & \cdots & \hat{X}_{q-p+2} \\ \vdots & \vdots & & \vdots \\ \hat{X}_{q+p-1} & \hat{X}_{q+p-2} & \cdots & \hat{X}_q \end{bmatrix}^{-1} \begin{bmatrix} \hat{X}_{q+1} \\ \hat{X}_{q+2} \\ \vdots \\ \hat{X}_{q+p} \end{bmatrix} \tag{12}$$

The value of coefficient β is obtained similarly. As a result, the estimate value $\hat{X}_t$ of X_t at time t can be acquired. Actually, $\hat{X}_t$ is utilized to predict the network traffic in the next moment, but the value cannot be directly used for relay node selection. If the total bandwidth is denoted by B_{total}, the normalized available bandwidth of the network can be defined as B_a:

$$B_a = \frac{B_{total} - \hat{X}_t}{B_{total}} \tag{13}$$

The network traffic prediction can obtain the network resource usage in the next moment. But the data transmission capacity of segments cannot be determined by one index. In order to accurately evaluate the node performance, the link delay, bandwidth and link connection time should also be comprehensively taken into consideration.

Link Delay: Without considering the time taken by the signal transmission and reception, the time taken by transmitting the information from the device to the relay node is assumed as the link delay $d_{iE}(t)$:

$$d_{iE}(t) = \frac{\sqrt{(x_E(t) - x_i(t))^2 + (y_E(t) - y_i(t)) + (z_E(t) - z_i(t))^2}}{c} \tag{14}$$

where $(x_i(t),\ y_i(t), z_i(t))$ and $(x_E(t),\ y_E(t), z_E(t))$ respectively represent the three-dimensional coordinates of relay node E and device i, and they are all functions of time. c is the speed of light. The value of $d_{iE}(t)$ is denoted by D_{iE}

Bandwidth: The data transmission rate always depends on the bandwidth provided by the node's transceiver and the unit is Mbps. For example, the total bandwidth B_{Etotal} of relay node E is 20 Mbps, and 5 Mbps has been used to forward other tasks. Meanwhile, the transceiver capacity B_{itotal} of device i is 18 Mbps. If the communication link is established between E and i, the maximum available bandwidth B_{Ei} is 15 Mbps, which is the smaller available Bvalue for both nodes:

$$B_{Ei} = \min(B_E,\ B_i) \tag{15}$$

where the value of B_{Ei} can be used to describe the bandwidth of device i.

Connection Time: The link connection time starts with the establishment of transmission links and ends with the satellites disappeared, where the disappearance means that two nodes have lost their physical visibility. It depends on the relative position of satellites, ground targets, and the Earth. The critical time when link establishment is defined as T_0 and when two nodes lose physical visibility is $T_{\max}$. The link connection time T_{Ei} between relay node E and device i can be expressed as:

$$T_{Ei} = T_{\max} - T_0 \tag{16}$$

For convenient comparison with the other indicators, we normalize B_a as B_a^*, D_{iE} as D_{iE}^*, B_{iE} as B_{iE}^*, T_{iE} as T_{iE}^*:

$$B_a^* = B_a \times 100 \tag{17}$$

$$D_{iE}^* = \frac{D_{iE} - D_{\min}}{D_{\max} - D_{\min}} \times 100 \tag{18}$$

$$B_{iE}^* = \frac{B_{iE} - B_{\min}}{B_{\max} - B_{\min}} \times 100 \tag{19}$$

$$T_{iE}^* = \frac{T_{iE} - T_{\min}}{T_{\max} - T_{\min}} \times 100 \tag{20}$$

where $D_{\max}$ and $D_{\min}$, $B_{\max}$ and $B_{\min}$, $T_{\max}$ and $T_{\min}$ are the maximum and minimum values in the dataset. Finally, the dataset can be expressed as X:

$$X = \{x_1, x_2, \ldots, x_n\} \tag{21}$$

where x_i is a 4-dimensional vector that represents the four characteristics of node i.

Utilizing the four parameters, the performance of the node can be evaluated. However, the calculation is too complex because the parameters are not independent of each other and require further processing. Therefore, it is necessary to find efficient and rapid evaluation methods. The Adaboost classifier is as an adaptive classifier. It trains a series of weak classifiers and combining them into a strong classifier to quickly meet the classification requirements of datasets in different dimensions, as shown in Fig. 1. Dataset X is divided into $N+P$ values. The dataset $y_1, y_2, \cdots, y_N, \cdots, y_{N+P}$ are

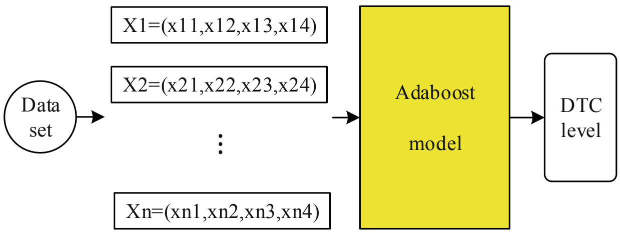

Fig. 1. The Adaboost model for relay node selection.

calculated as classification labels of nodes. Finally, the dataset T is obtained:

$$T = \{(X_1, y_1), (X_2, y_2), \cdots, (X_{N+P}, y_{N+P})\} \tag{22}$$

where $X_i \in \chi \subseteq N^n$, $y_i \in \{1, 2, 3, 4\}$. The first N sets of data are divided as the training set T_N, and the last P sets of data are used as the testing set T_P. The training set T_N is used to train the strong classifier as:

$$H_{final} = sign(f(x)) = sign\left(\sum_{t=1}^{T} \alpha_t H_t(x)\right) \tag{23}$$

According to the above, each node in SAGIN is classified to 1, 2, 3, 4 levels. The higher the level, the stronger the DTC. Meanwhile, the entire network topology can be described using the directed connected graph. For all nodes, there are:

$$IM = \left\{ \begin{array}{l} E_{11}, E_{12}, \ldots, E_{1j} \\ E_{21}, E_{22}, \ldots, E_{2j} \\ \ldots \\ E_{i1}, E_{i2}, \ldots, E_{ij} \end{array} \right\} \tag{24}$$

where the value of each E_{ij} is 1, 2, 3, or 4. The value expresses the DTC of link between node i and node j. If two nodes have no physical visibility, the value is 0. It only needs to select the nodes with the optimal level to form the data transmission links (DTL), as shown in Fig. 2. The important value of ALP is that it has low computational complexity. Further, it can promote the load balance of the whole SAGIN, so as to prevent the link congestion caused by segment overload.

3 Simulation Analysis

The simulation is carried out over a predictable three-layer SAGIN network with the use of the Satellite Tool Kit (STK) simulator. The LEO satellite model is established with reference to iridium constellation. 30 ground devices and 20 UAVs are deployed at Chengdu city in STK simulator. Since traffic data of SAGIN network cannot be obtained, this paper will use the dataset in [6] for traffic prediction, where the authors have proved the reasonability and self-similarity of the traffic data. Each link of the

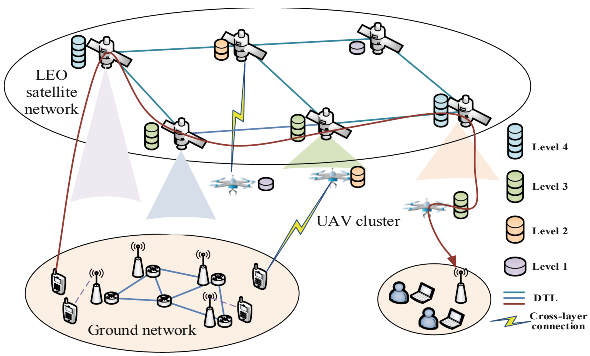

Fig. 2. The relay node selection according to available capacity levels.

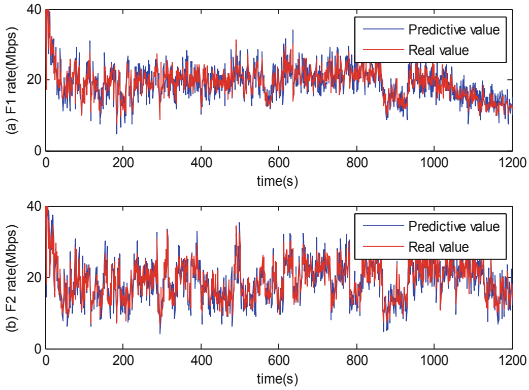

Fig. 3. Prediction results of network traffic flow F1 and F2.

SAGIN scenario corresponds to an origin destination (OD) flow in the dataset. Then we connect STK with MATLAB to obtain the other network data including link delay, bandwidth, and connection time. The calculation and comparison of the proposed scheme and other methods are also carried out in MATLAB. In the simulation scenario, each device is covered by multiple UAVs and LEO satellites in each time slot.

In the simulation, we first analyze the traffic prediction results. Figure 3 shows the prediction results of network traffic flows F1 and F2. In our simulation tests, other end-to-end traffic pairs holds similar results. As shown in Fig. 3(a) and (b), the real network traffic exhibits significant time-varying characteristics under different time slots. The ARMA model can capture dynamic changes of the network traffic flow F1 and F2 effectively. Although there are errors, we have seen that the ARMA model can better look for the traffic trends. These further indicates that the utilized ARMA model can effectively predict the change of the network traffic over the time.

Next we discuss the classification results of the Adaboost model. 50 data sets is selected randomly, 30 for training, 20 for testing. Figure 4(a) express the change of classification error (CE) in model training stage. It can be seen form Fig. 4(a) that the CE shows a downward trend as the weak classifier number increases, from 20% in 1 weak classifier to 0% in 18 weak classifier. The classification results of different capacity levels is expressed in Fig. 4(b). It can be seen that each set of data was classified to the correct level. This reflects that the training model is effective.

Figure 5 expresses the training results of Adaboost model with different training samples and different dataset proportions. Figure 5(a) and (b) respectively use 25 training data and 100 training data. It can be seen that Fig. 5(a) utilize 18 weak classifiers to reduce the CE to 7%, while Fig. 5(a) makes use of 20 weak classifiers to reduce the CE to 5%. It can be found that more training samples need more weak classifiers to complete feature recognition so as to achieve better classification accuracy. Particularly, the CE may fluctuate when the training samples are small. Therefore, the training sample with 50 data sets is enough to meet the requirements of Adaboost model training. Different proportions of training and test data may also affect the accuracy of the Adaboost model. Figure 5(c)–(d) represent the model training results

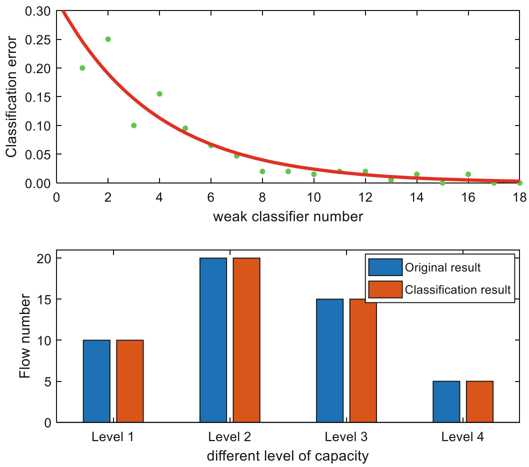

Fig. 4. The classification result of ALP algorithm.

under different proportions in 50 data sets. It can be found that the classification result is better when the proportion of training set is higher. But this may also produce unreliable models because of less test data. However, if the training set is reduced, the stability of the model will be challenged. Therefore, after comprehensive consideration, we select the Adaboost model with the best accuracy, including 30 training data and 20 test data. The remaining nodes in SAGIN are classified by this model.

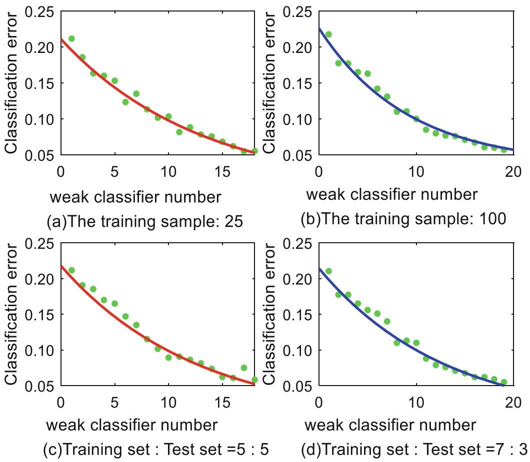

Fig. 5. The impact of sample size and proportion on classification error.

Next, we will evaluate the proposed ALP scheme in terms of link congestion, compared with current mainstream link construction schemes including the shortest path Dijkstra algorithm (SPDA) and the traveling salesman algorithm (TSA). We define the sum of overloads of all nodes in one link as the link congestion, and examine three schemes. Figure 6 displays the link congestion of three schemes with the increase of number of tasks. It can be seen that the SPDA method has the fastest increase in link congestion value, followed by TSA method, and ALP method has the slowest growth. This is because the node with the largest available capacity is considered first in ALP. The other two schemes put the shortest path in the first place and rarely consider the link congestion. As a result, it is easy to cause link congestion and serious packet loss, affecting the quality of data transmission. So the communications link of ALP scheme is relatively unimpeded.

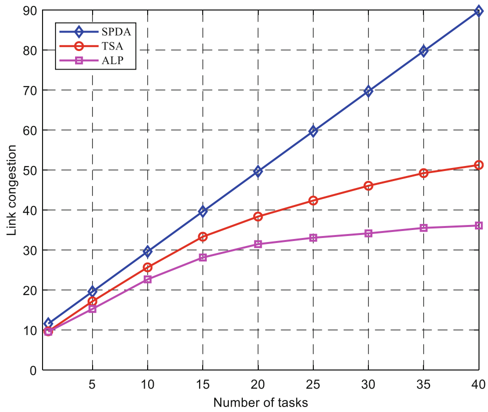

Fig. 6. The comparison of link congestion.

4 Conclusion

This paper studies the relay node selection problem in the Space-air-ground integrated network (SAGIN). In contrast to the previous studies, we jointly consider traffic prediction and segment classification in SAGIN. We utilize the autoregressive moving average (ARMA) model for traffic prediction, and the results of prediction are imported the Adaboost model with other link performances to realize the classification of involved nodes. The simulation results show that the proposed relay node selection scheme is promising.

Acknowledgment. This work was supported by National Natural Science Foundation of China (No. 61571104), Sichuan Science and Technology Program (No. 2018JY0539), Key projects of the Sichuan Provincial Education Department (No. 18ZA0219), Fundamental Research Funds for the Central Universities (No. ZYGX2017KYQD170), and Innovation Funding (No. 2018510 007000134). The authors wish to thank the reviewers for their helpful comments.

References

1. Liu, J., Shi, Y., Fadlullah, Z.M., et al.: Space-air-ground integrated network: a survey. IEEE Commun. Surv. Tutor. **20**(4), 2714–2741 (2018)
2. Liu, Y., Xu, W., Tang, F., et al.: An improved multi-path routing algorithm for hybrid LEO-MEO satellite networks. In: Proceedings of ISPA 2016, pp. 1101–1105 (2016)
3. Zhang, Z., Jiang, C., Guo, S., et al.: Temporal centrality-balanced traffic management for space satellite networks. IEEE Trans. Veh. Technol. **67**(5), 4427–4439 (2018)
4. Araniti, G., Bisio, I., De Sanctis, M., et al.: Multimedia content delivery for emerging 5G-satellite networks. IEEE Trans. Broadcast. **62**(1), 10–23 (2016)
5. Han, Y., Li, D., Guo, Q.: Self-similar traffic prediction scheme based on wavelet transform for satellite internet services, In: Proceedings of MLICOM 2016, pp. 189–197 (2016)
6. Zhou, D., Sheng, M., Wang, X., et al.: Mission aware contact plan design in resource-limited small satellite networks. IEEE Trans. Commun. **65**(6), 2451–2466 (2017)
7. Wang, Y., Sheng, M., Li, J., et al.: Dynamic contact plan design in broadband satellite networks with varying contact capacity. IEEE Commun. Lett. **20**(12), 2410–2413 (2016)
8. Jiang, D., Wang, W., Shi, L., et al.: A compressive sensing-based approach to end-to-end network traffic reconstruction. IEEE Trans. Netw. Sci. Eng. **5**(3), 1–12 (2018)
9. Jiang, D., Huo, L., Li, Y.: Fine-granularity inference and estimations to network traffic for SDN. PLoS ONE **13**(5), 1–23 (2018)
10. Jiang, D., Lv, Z., Huo, L., et al.: A joint multi-criteria utility-based network selection approach for vehicle-to-infrastructure networking. IEEE Trans. Intell. Transp. Syst. **99**, 1–15 (2018). (SCI, EI)
11. Jiang, D., Zhang, Y., Song, H., et al.: Intelligent optimization-based energy-efficient networking in cloud services for multimedia big data. In: Proceedings of IPCCC 2018, pp. 1–6 (2018)
12. Jiang, D., Huo, L., Song, H.: Understanding base stations' behaviors and activities with big data analysis. In: Proceedings of Globecom 2018, pp. 1–7 (2018)